Extremely robust and conformable capacitive pressure sensors based on flexible polyurethane foams and stretchable metallization

H. Vandeparre, D. Watson, and S. P. Lacour

Citation: Applied Physics Letters **103**, 204103 (2013); doi: 10.1063/1.4832416
View online: http://dx.doi.org/10.1063/1.4832416
View Table of Contents: http://scitation.aip.org/content/aip/journal/apl/103/20?ver=pdfcov
Published by the AIP Publishing

Extremely robust and conformable capacitive pressure sensors based on flexible polyurethane foams and stretchable metallization

H. Vandeparre, D. Watson, and S. P. Lacour[a)]
Ecole Polytechnique Fédérale du Lausanne (EPFL) Centre for Neuroprosthetics, STI / IMT/IBI / LSBI, CH-1015 Lausanne, Switzerland

(Received 20 September 2013; accepted 28 October 2013; published online 14 November 2013)

Microfabricated capacitive sensors prepared with elastomeric foam dielectric films and stretchable metallic electrodes display robustness to extreme conditions including stretching and tissue-like folding and autoclaving. The open cellular structure of the elastomeric foam leads to significant increase of the capacitance upon compression of the dielectric membrane. The sensor sensitivity can be adjusted locally with the foam density to detect normal pressure in the 1 kPa to 100 kPa range. Such pressure transducers will find applications in interfaces between the body and support surfaces such as mattresses, joysticks or prosthetic sockets, in artificial skins and wearable robotics.
 [http://dx.doi.org/10.1063/1.4832416]

Pressure is measured in a variety of applications ranging from product manufacturing, object recognition to medical research. It is a fundamental metric for tactile interfaces. Discrete pressure sensors produced with MEMS technology are widely available today but cannot be easily distributed in a large-area skin-like format. Several groups have recently reported artificial tactile skins for applications in macroelectronics, soft robotics, prosthetics, and bio-inspired electronics. These "soft" pressure sensing technologies rely on microstructured elastomers[1,2] or composite polymers[3–5] integrated in resistive or capacitive devices, ferroelectric sensors,[6] liquid metal microfluidics,[7] optical waveguides[8,9] or inorganic semiconductor nanomembranes printed on elastomeric substrate.[10]

In all cases, the soft polymer is implemented as the carrier or the sensitive material and is usually a homogeneous elastomer with an elastic modulus in the 10 s–1000 s kPa range. In this paper, we explore how microcellular elastomer foams can be implemented for soft pressure sensing skins and demonstrate highly deformable yet reliable capacitive sensors. The foam sensors employ stretchable thin gold film electrodes separated by a dielectric membrane of flexible polyurethane (PU) foam. Fig. 1(a) illustrates the robustness and deformability of the sensor skin, which can withstand crumpling, sharp indentation, and autoclaving without deterioration of its electromechanical performance.

The soft sensing skin is prepared on a flexible, microcellular, open-cell polyurethane foam. The two-component elastomer is mechanically mixed and allowed to foam up, producing membranes with selected density and fairly uniform cell size.[11] Evaporating thin (<100 nm thick) gold layers onto the foam elastomer produces highly stretchable metallization. The open-cell foam structure conveys highly anisotropic mechanical properties to the metallic coating. Upon stretching, large strain fields inducing cracks and folds in the metal film only localize above the foam's cells, while the surrounding ligaments remain almost strain-free, enabling stable electrical conduction in the metal film.[11] The initial electrical resistivity of the thin gold film on PU foam is 10 $\mu\Omega$ cm, similar to that of gold film on polyDimethyl siloxane (PDMS).[12]

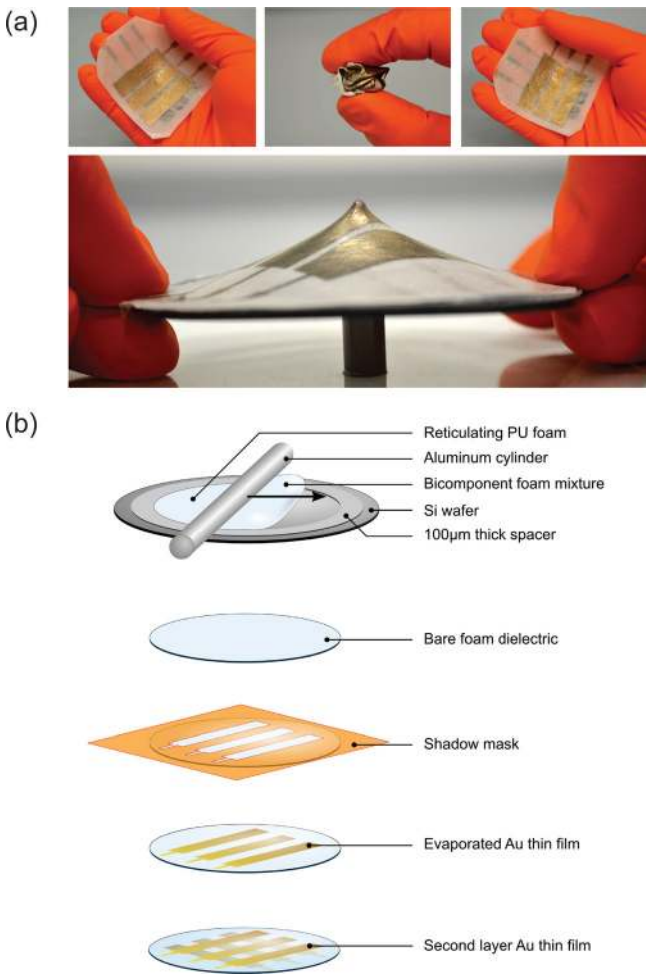

FIG. 1. (a) Pictures of a highly compliant and robust sensor skin prepared with flexible polyurethane foam and stretchable thin film metallization. The skin can sustain crumpling as well as sharp indentation (bottom picture). The gold film coating remains intact. (b) Pressure sensor skin fabrication process.

[a)]Author to whom correspondence should be addressed. Electronic mail: stephanie.lacour@epfl.ch.

The process flow used to prepare the soft pressure sensing skin is presented in Fig. 1(b). First, a two-component mixture of flexible polyurethane foam (Smooth-on Flex-Foam-iT, grades III or 17) is dispensed on a glass wafer and bar-coated to the desired thickness. After 2 h crosslinking at room temperature, the foam top surface is coated with an array of electrodes, typically a 25 nm thick film of evaporated gold on top of a 5 nm thick adhesion layer of titanium patterned through a shadow mask as three parallel stripes of 1 cm width and 5 cm length (Fig. 1(a)). The metallized foam is then flipped and coated using the same process with a second array of electrodes positioned at a 90° angle relative to the top electrodes.

Fig. 2(a) displays compressive stress-strain curves for low (0.1 g cm^{-3}) and medium (0.4 g cm^{-3}) density flexible polyurethane foam membranes compressed at a constant rate of 15 μm min^{-1}. Under in-plane compression, the open-cell flexible foam exhibits three deformation regimes: linear elastic, plateau, and densification.[13] At small displacements, bending of the cell walls results in linear elasticity. The transition from linear to non-linear behavior occurs at a moderate strain associated with elastic (reversible) buckling of the cell walls. The long collapse plateau is characterized by a nearly constant stress across a wide range of compressive strains. The transition to densification occurs at a strain, where most of the porosity has been squeezed out and dramatic stiffening of the elastomer occurs. Changing the foam density modifies drastically the stress-strain curve: increasing the film density from 0.1 to 0.4 g/cm^3 stiffens the polymer (the elastic modulus (E*) rises from 20 to 760 kPa), shortens the stress plateau, and finally reduces the strain at which densification starts.

The foam relative permittivity can be calculated according to Eq. (1)

$$\varepsilon^* = 1 + (\varepsilon_{s,PU} - 1)\frac{\rho^*}{\rho_{PU}}, \tag{1}$$

where $\varepsilon_{s,PU}$, ρ_{PU}, and ρ^* are the bulk PU permittivity (=3.5), the bulk PU density (=1.2 g/cm^3), and the foam density, respectively. The stiff foam ($\rho^* = 0.4\,\mathrm{g\,cm^{-3}}$) has a larger volume fraction of polyurethane domains relative to that of voids compared to soft foams ($\rho^* = 0.1\,\mathrm{g\,cm^{-3}}$) therefore its initial permittivity is larger: $\varepsilon^*_{stiff} = 1.83$ and $\varepsilon^*_{soft} = 1.21$. Figs. 3(b) and 3(c) show the capacitance and deducted relative permittivity across the foam membranes placed in an Agilent 16451B dielectric test fixture. The 8 mm diameter soft and stiff foam membranes are 440 and 690 μm thick, respectively; electrodes are 5 mm diameter. The applied compression is controlled with a micrometer screw. Stray capacitances can be neglected using a guard electrode montage in the top plate electrode. For a given compression, the soft foam displays a larger increase in capacitance than the stiff foam; the capacitance increase in bulk polyurethane is comparatively modest. When the mechanical load is applied to the foam, air is expelled through the open-cell structure leading to a denser material and an increased ε^*. The latter increases to a maximum corresponding to the compressive stress plateau. In this regime, the porosity is easily removed from the foam microstructure. At high compressive strain (>0.5), densification starts from

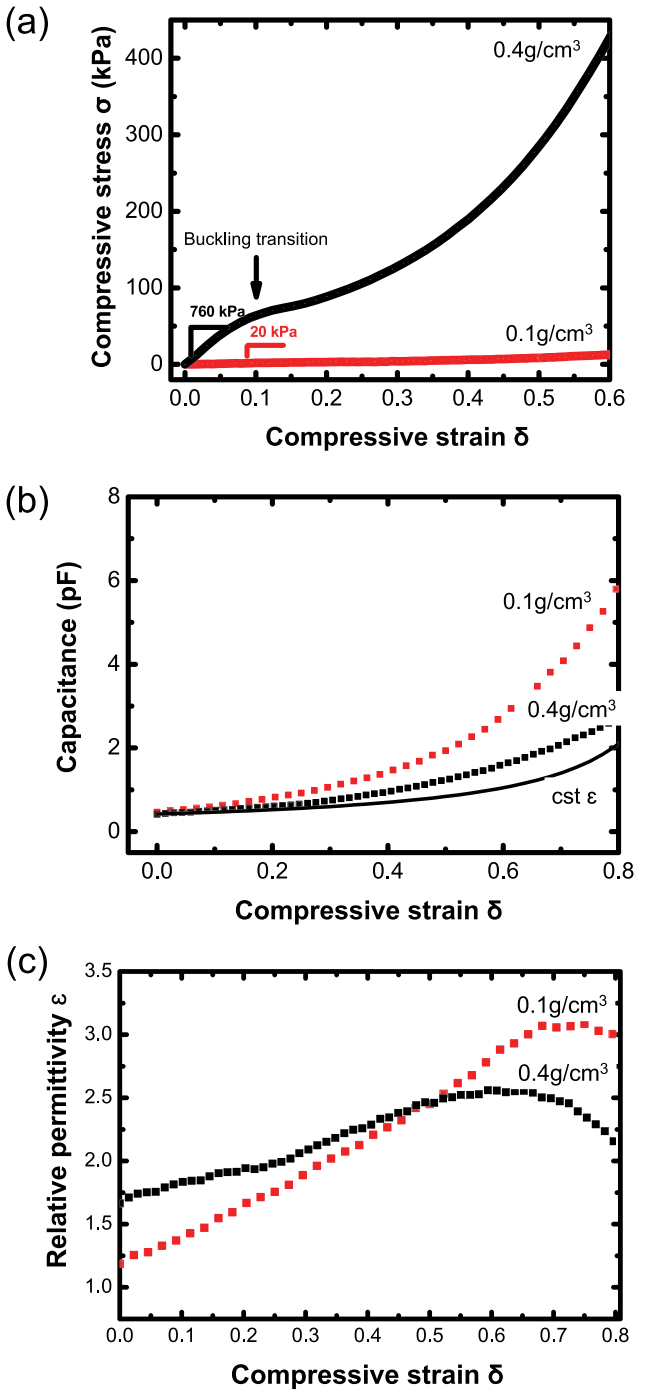

FIG. 2. Mechanical and dielectric properties of the flexible polyurethane foam membranes. (a) Compressive stress-strain response of a soft (0.1 g/cm^3) and stiff (0.4 g/cm^3) foam. (b) Plate capacitance measured across bare (uncoated) foam membranes as a function of applied compression (dotted curves) and calculated using a constant relative permittivity ($C = \varepsilon^* \varepsilon_0 A/t$, plain curve). (c) Corresponding relative permittivity as a function applied strain.

contact between the cell walls.[13] The strain at which ε^* reaches the maximum is directly related to the foam density. An increased foam density leads to thicker cell walls, which touch at smaller strains, reducing in the meantime the strain at which densification starts and ε^* peaks. A decrease from 0.75 to 0.6 strains is indeed observed when increasing the foam density from 0.1 to 0.4 g/cm^3 (Fig. 3(c)). Furthermore, in the densification regime, the fall in relative permittivity may be explained by the difficulty in further removing the

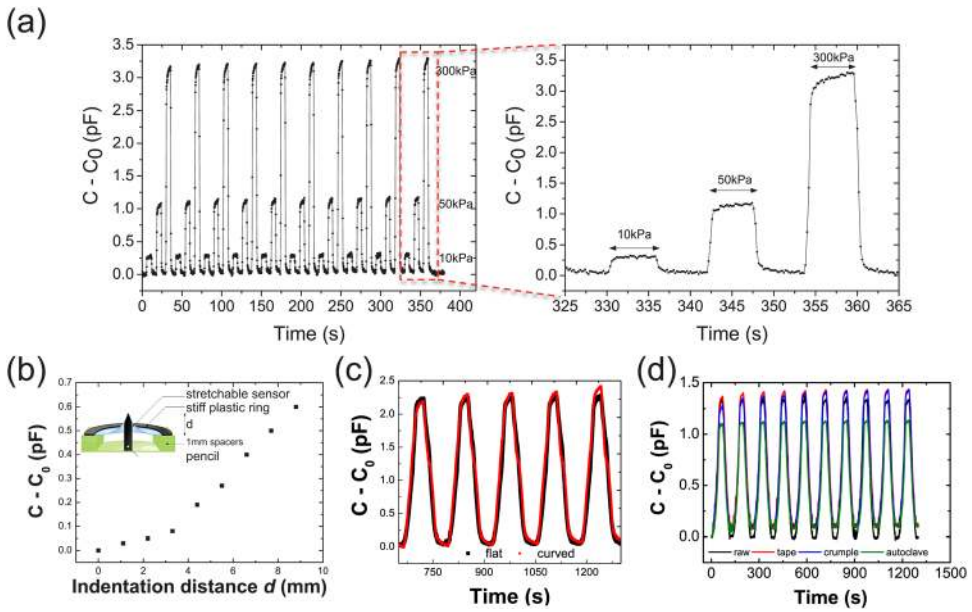

FIG. 3. Soft foam sensor response (a) to cyclic indentation, (b) to sharp indentation, and (c) before and during shaping over a golf ball over 5 cycles to 75% compressive strain. (d) Cyclic sensor response to 75% compression before and after exposure to tape test, crumpling and autoclaving. All sensors are 1 cm^2.

residual porosity: PU cell walls compress locking in the pore space.[14]

Figure 3 summarizes the responses to compressive loadings of capacitive foam sensors. The sensors are prepared (as described in Fig. 1(b)) by using the soft polyurethane foam ($\rho^* = 0.1\,g\,cm^{-3}$, 440 μm thick) which gives the highest pressure sensitivity; each sensor has a 1 cm^2 electrode surface area. The sensor capacitance, $C = \varepsilon^* \varepsilon_0 \frac{A}{t}$, is recorded with an E4980A Agilent inductance capacitance resistance (LCR) meter; compression is applied with a motorized indenter (a 5 mm diameter plastic indenter moving at a 15 μm/s rate). Fig. 3(a) illustrates the net change in capacitance of the sensor during cyclic deformation to 10 kPa, 50 kPa, and 300 kPa, (indenting over 1 s and pausing 5 s); each cycle (with 3 applied pressures) lasts 46 s. The sensor response is relatively fast (in the 100 ms range) and independent on the range of applied pressure.

Fig. 3(b) plots the sensor response, while the sensor skin is conformed over the tip of a pencil. The skin is held in a plastic ring (10 cm diameter) for easy manipulation and the pencil tip, normal to the skin plane, is centered on the 1 cm^2 sensor (Fig. 3(b) inset). Using a manual stage, the pencil tip slowly indents the back of the skin, which was preliminary coated with a protective 100 μm thick silicone membrane. First, the capacitance changes little with the depth of indentation due to the silicone damping and the small contact area with the pencil tip. Further indentation linearly increases the capacitance as the skin uniformly coats the sides of the pencil tip. After removal of the indenter, the gold film surface is intact, and the sensor capacitance recovers its initial value.

The sensor skin is then coated over a golf ball. Typical responses of the measured change in sensor capacitance as a function of time are shown in Fig. 3(c): the sensor matrix is held flat (prior to conforming the ball) then fitted to the ball. As a cyclic, 75% compressive strain is applied to the surface of the foam sensor, its capacitance repeatably increases by 2.25 pF. Stretching the skin over the ball leads to a change of the capacitance at rest, C_0, from 4.7 pF to 6.5 pF, but the temporal response and capacitance *deltas* are not otherwise altered by the imposed multi-axial stretch.

We evaluated the robustness of the foam sensor technology by recording the sensor response prior to and immediately after three demanding treatments. Fig. 3(d) shows the cycling response of a sensor before and after being subjected to, in sequence, the scotch-tape test (sticking and peeling off of scotch tape on the metal film), crumpling (as shown in Fig. 1(a)), and autoclaving (121 °C, 200 kPa, 20 min.). Compressive cycles to 75% strain are applied with the 5 mm diameter indenter on the surface of the sensor mounted flat in the experimental setup. The sensor response is surprisingly stable. Only autoclaving significantly affects the response, yet does not annihilate it.

The foam sensor skin fabrication process may be simply altered to pattern distributed sensing volumes of selected stiffness within a single foam membrane (Fig. 4(a)). Before metallization, the flexible foam membrane is perforated to produce an array of holes that are subsequently filled with softer foam. A thin residual layer of the softest foam also coats the whole skin surface as shown in Fig. 4(a). Electrodes are then aligned with the soft and hard foam patterns, resulting in sensors of two different stiffnesses and sensitivities side-by-side and on the same substrate (Fig. 4(b)). Large sensors (1 cm^2 surface area) are presented here but smaller features may be patterned using laser cutting or molding against three-dimensional negative structures. Figs. 4(a) and 4(d) show a photograph and the response of the hybrid sensor skin. The soft sensors are significantly more sensitive than those patterned on the stiff foam, registering changes in capacity of 0.015 pF/kPa vs 0.0026 pF/kPa in the initial linear regime. In addition, as a byproduct of the fabrication process, the entire array is coated with a thin layer of soft foam. This improves the sensitivity of the stiff sensors in the low pressure range without affecting its response in the high-pressure range.

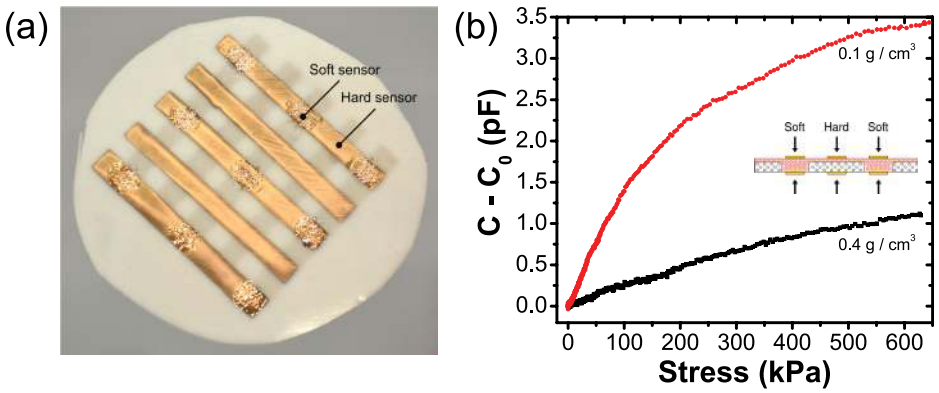

FIG. 4. (a) Picture of a hybrid foam sensor skin (each gold stripe is 1 cm wide). (b) "Stiff" and "soft" sensor response as a function of applied pressure.

In summary, we demonstrated a straightforward approach to design and fabricate highly robust and compliant pressure sensors using flexible elastomeric foams. The microcellular structure combined with the elastic polymer matrix conveys improved mechanical, and as a result, electromechanical properties compared to bulk elastomers. The pressure sensitivity and operating range of the foam-based sensors may be adjusted by modulating the foam density. Flexible foams are already available in a wide range of formats, materials, and stiffness and are used in industrial as well as biomedical settings. Their compatibility with thin film metallization opens the path to the production of large-area, lightweight, and low-cost sensory skin.

We acknowledge the support from the European Research Council through an ERC Starting Grant No. 259419-ESKIN and the Bertarelli Foundation.

[1]G. Schwartz, B. C.-K. Tee, J. Mei, A. L. Appleton, D. H. Kim, H. Wang, and Z. Bao, Nature Commun. **4**, 1859 (2013).
[2]C. Pang, G.-Y. Lee, T.-i. Kim, S. M. Kim, H. N. Kim, S.-H. Ahn, and K.-Y. Suh, Nature Mater. **11**, 795–801 (2012).
[3]T. Someya, T. Sekitani, S. Iba, Y. Kato, H. Kawaguchi, and T. Sakurai, Proc. Natl. Acad. Sci. U.S.A. **101**(27), 9966–9970 (2004).
[4]W. Hu, X. Niu, R. Zhao, and Q. Pei, Appl. Phys. Lett. **102**, 083303 (2013).
[5]H.-B. Yao, J. Ge, C.-F. Wang, X. Wang, W. Hu, Z.-J. Zheng, Y. Ni, and S.-H. Yu, "A Flexible and Highly Pressure-Sensitive Graphene–Polyurethane Sponge Based on Fractured Microstructure Design," Adv. Mater. (published online).
[6]I. Graz, M. Kaltenbrunner, C. Keplinger, R. Schwödiauer, S. Bauer, S. P. Lacour, and S. Wagner, Appl. Phys. Lett. **89**, 073501 (2006).
[7]R. K. Kramer, C. Majidi, R. Sahai, and R. J. Wood, IEEE/RSJ International Conference on Intelligent Robots and Systems, San Francisco (IEEE, 2011), pp. 1919–1926.
[8]M. Ramuz, B. C.-K. Tee, J. B.-H. Tok, and Z. Bao, Adv. Mater. **24**(24), 3223–3227 (2012).
[9]J. Missinne, G. V. Steenberge, B. V. Hoe, K. V. Coillie, T. V. Gijseghem, P. Dubruel, J. Vanfleteren, and P. V. Daele, "An array waveguide sensor for artificial optical skins," Proc. SPIE **7221**, 722105 (2009).
[10]D.-H. Kim, N. Lu, R. Ghaffari, Y.-S. Kim, S. P. Lee, L. Xu, J. Wu, R.-H. Kim, J. Song, Z. Liu, J. Viventi, B. D. Graff, B. Elolampi, M. Mansour, M. J. Slepian, S. Hwang, J. D. Moss, S.-M. Won, Y. Huang, B. Litt, and J. A. Rogers, Nature Mater. **10**, 316–323 (2011).
[11]H. Vandeparre, Q. Liu, I. R. Minev, Z. Suo, and S. P. Lacour, Adv. Mater. **25**(22), 3117–3121 (2013).
[12]S. P. Lacour, J. E. Jones, S. Wagner, T. Li, and Z. Suo, Proc. IEEE **93**(8), 1459–1467 (2005).
[13]L. J. Gibson and M. F. Ashby, *Cellular Solids - Structures and Properties* (Cambridge University Press, 1999).
[14]A. D. Brydon, S. G. Bardenhagen, E. A. Miller, and G. T. Seidler, J. Mech. Phys. Solids **53**, 2638–2660 (2005).